

**INF 5300, spring 2008:**

# **OBJECT SHAPE DESCRIPTORS**

## **Area, perimeter, compactness, and spatial moments**

Assuming that we have a segmented and labeled image, i.e. each object that is to be described has been identified. How do we then obtain a numerical description of the geometrical shape of each object, so that a later classification stage may distinguish between different classes of object shapes, without knowing in advance what characteristic shape features that are present in the different objects that are present in this particular set of images?

This seems to be a difficult problem, and solutions may be divided into two separate branches:

- One is the strictly mathematical category, using e.g. orthogonal spatial moments to obtain an (almost) infinite sequence of features that is uniquely determined by the object, and that conversely determines the object.
- The other approach is based on finding a quick and simple solution that works, and has resulted in a lot of useful, application-dependent heuristics.

There is no generally accepted methodology for shape description, but it is reasonable to state that the location and direction of high curvature in the outer boundary of the object carries essential information.

## 1 Basic region descriptors

If we let  $A$  be the area and  $P$  be the perimeter, i.e., the length of the outer contour of a planar object, the circularity is defined by  $C = 4\pi A/P^2$ . In the continuous image domain  $C$  is 1 for a perfect circle and between 0 and 1 for all other shapes. Even in discretized images, these three parameters are useful features to describe the shape of a 2D object.

### 1.1 Area and perimeter

The very simplest parameter of a region or an object in an image is its area. Generally, the area is defined as

$$A = \iint_{x,y} I(x,y) dx dy$$

where  $I(x,y) = 1$  if the pixel is within the object, and 0 otherwise. In digital images, integrals are approximated by summations, so

$$A = \sum_x \sum_y I(x,y) \Delta A$$

Where  $\Delta A$  is the area of one pixel, so that if  $\Delta A = 1$ , then the area is simply measured in pixels. The area will obviously change if we change the scale of the image, although the change is not perfectly linear, because of the discretization of the image. Intuitively, the area should be invariant to rotation of the object. However, small errors will occur when applying a rotation transformation owing to the discretization of pixels in the image.

Estimating the perimeter of an object in a digital image is a problem, since the length of the original contour may be considerably different from the length of the digital contour. It is impossible to reconstruct a “true” continuous contour from discrete data, because many possible contours, having different lengths, correspond to a particular discrete realization. Therefore, some reasonable assumptions must be made. Separate length estimators exist for straight line segments and circular arcs, and at least one estimator seems to be accurate for both. Ideally, one would like to achieve a precise, efficient and simultaneous computation of object area and object perimeter.

### 1.1.1 Bit quads

Matching each small region in a binary image with some pixel patterns and counting the number of matches for each pattern, the object area and perimeter may be formulated as weighted sums of the different counts. Let  $n\{Q\}$  be the number of matches between the image pixels and the pattern  $Q$ . By this simple definition, the area and perimeter of a 4-connected object is given by

$$A = n\{1\}, \quad P = 2n\{0 \ 1\} + 2n\left\{\begin{matrix} 0 \\ 1 \end{matrix}\right\}$$

A set of 2 x 2 pixel patterns called Bit Quads, given to the right, handle 8-connected images. Gray (1971) computed the area and the perimeter of the object as

$$A_G = \frac{1}{4} [n\{Q_1\} + 2n\{Q_2\} + 3n\{Q_3\} + 4n\{Q_4\} + 2n\{Q_D\}]$$

$$P_G = n\{Q_1\} + n\{Q_2\} + n\{Q_3\} + 2n\{Q_D\}$$

These formulas may be in considerable error compared to the true values for continuous objects that have been discretized. More accurate formulas were given by Pratt (1991) from a note by Duda :

$$A_D = \frac{1}{4} \left[ n\{Q_1\} + 2n\{Q_2\} + \frac{7}{2}n\{Q_3\} + 4n\{Q_4\} + 3n\{Q_D\} \right]$$

$$P_D = n\{Q_2\} + \frac{1}{\sqrt{2}} [n\{Q_2\} + n\{Q_3\} + 2n\{Q_D\}]$$

$$Q_0: \begin{bmatrix} 0 & 0 \\ 0 & 0 \end{bmatrix}$$

$$Q_1: \begin{bmatrix} 1 & 0 \\ 0 & 0 \end{bmatrix} \begin{bmatrix} 0 & 1 \\ 0 & 0 \end{bmatrix} \begin{bmatrix} 0 & 0 \\ 0 & 1 \end{bmatrix} \begin{bmatrix} 0 & 0 \\ 1 & 0 \end{bmatrix}$$

$$Q_2: \begin{bmatrix} 1 & 1 \\ 0 & 0 \end{bmatrix} \begin{bmatrix} 0 & 1 \\ 0 & 1 \end{bmatrix} \begin{bmatrix} 0 & 0 \\ 1 & 1 \end{bmatrix} \begin{bmatrix} 1 & 0 \\ 1 & 0 \end{bmatrix}$$

$$Q_3: \begin{bmatrix} 1 & 1 \\ 0 & 1 \end{bmatrix} \begin{bmatrix} 0 & 1 \\ 1 & 1 \end{bmatrix} \begin{bmatrix} 1 & 0 \\ 1 & 1 \end{bmatrix} \begin{bmatrix} 1 & 1 \\ 1 & 0 \end{bmatrix}$$

$$Q_4: \begin{bmatrix} 1 & 1 \\ 1 & 1 \end{bmatrix}$$

$$Q_D: \begin{bmatrix} 1 & 0 \\ 0 & 1 \end{bmatrix} \begin{bmatrix} 0 & 1 \\ 1 & 0 \end{bmatrix}$$



### 1.1.3 Area from contour

As we have seen, the area of a binary object may be obtained either by counting the number of pixels within the object, as a weighted sum of bit-quad pattern matches. From calculus we know that the surface integral over a region  $S$  having a contour  $C$  is given by Green's theorem. Thus:

$$A = \iint_S dx dy = \int_C x dy$$

A pseudo-code for this integration in a discrete image may look like this:

```

s := 0.0;
n := n + 1;
pkt[n].x := pkt[1].x;
pkt[n].y := pkt[1].y;
for i:=2 step 1 until n do
begin
    dy := pkt[i].y - pkt[i-1].y
    s := s + (pkt[i].x + pkt[i-1].x)/2 * dy;
end;
area := if (s > 0) then s else -s;

```

But instead of performing the summation over absolutely every object contour pixel, an approximate area may be obtained from the (x,y)-coordinates of  $N$  polygon vertices:

$$\hat{A} = \frac{1}{2} \left| \sum_{k=0}^{N-1} (x_k y_{k+1} - x_{k+1} y_k) \right|$$

where the sign of the sum reflects whether we have followed the object contour in the clockwise or anti-clockwise direction.

Obviously, the precision of this approximation depends entirely on how well the polygonization of the discretized contour approximates the contour.

### 1.1.4 Recursive and sequential polygonization of boundary

We may restrict the polygonization to obtaining a subset of the original set of boundary points, in such a way that the polygon line segments do not deviate more than a certain amount from the curve formed by a sequence of line segments joining the original boundary points.

The original recursive boundary splitting algorithm of Douglas and Peucker (1973) goes as follows: Draw a straight line segment between the pair of contour points that have the greatest internal distance. These two points are the initial breakpoints.

- For each intermediate point: Compute the point-to-line distance, and find the point with the greatest distance from the line.

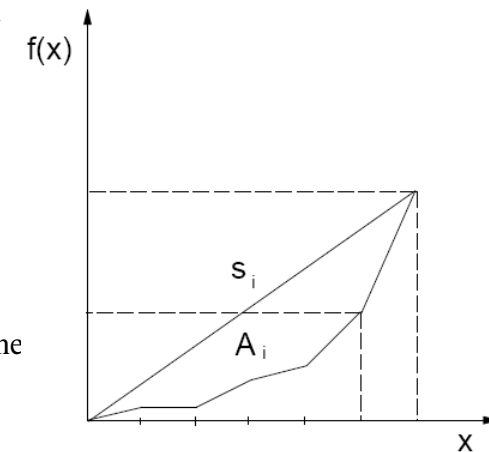
If this distance is greater than a given threshold, we have a new breakpoint between the two previous ones. The previous line segment is replaced by two, and the bullet-point above is repeated for each of them. The procedure is repeated until all contour points are within the threshold distance from a corresponding line segment. The resulting ordered set of breakpoints is then the set of vertices of a polygon approximating the original contour.

This algorithm, or variations on it, is probably the most frequently used polygonization method. Since it is recursive, the Euclidian distance from each boundary point to a new boundary approximating line segment has to be computed several times, so the procedure is fairly slow.

The sequential polygonization method of Wall and Danielsson (1984) may start any contour point. We then step from point to point through the ordered sequence of contour points, and outputs the previous point as a new breakpoint if the area deviation  $A$  per unit length  $s$  of the approximating line segment exceeds a pre-specified tolerance,  $T_{WD}$ .

- Using the previous breakpoint as the current origin, the area between the contour and the approximating line segment is accumulated by the equation to the right:
- If  $|A_i|/s_i < T$ ,  $i$  is incremented and  $(A_i, s_i)$  is recomputed.
- Otherwise, the previous point is stored as a new breakpoint, and the origin is moved.

This method is purely sequential and very fast. It can also be used for polygonization of 1D curves.



$$A_i = A_{i-1} + \frac{1}{2}(y_i x_{i-1} - x_i y_{i-1}), \quad s_i = \sqrt{x_i^2 + y_i^2}$$

### 1.1.5 A comparison of methods

Yang et al. (1994) tested the precision of the various methods by estimating the areas and perimeters of circles having an integer radius  $R$  from 5 to 70 pixels. Binary test images were generated by giving intensity values

$$g(x, y) = \begin{cases} 1 & \text{if } (x - x_0)^2 + (y - y_0)^2 \leq R \\ 0 & \text{otherwise} \end{cases}$$

The relative errors were defined as

$$\varepsilon = \frac{(\hat{x} - x)}{x}$$

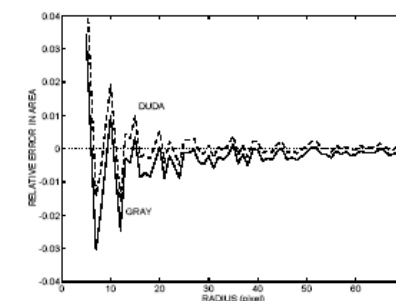
where  $x$  is the true value ( $A = \pi R^2$  and  $P = 2\pi R$ ).

From the top panel to the right we see that the area estimator of Duda is slightly better than that of Gray. The mid-crack method gave a result very similar to that of Gray. The Freeman method underestimated the area, giving a relative error similar to that of the Duda method if we assume that the radius is  $R-0.5$ .

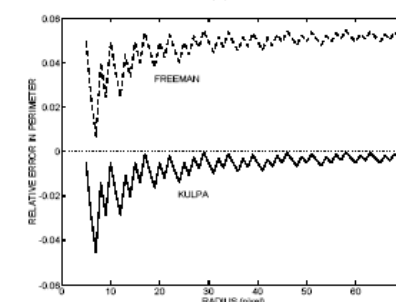
From the middle panel we see that Kulpa's perimeter is more accurate than Freeman's perimeter. Gray's perimeter gave a large overestimation. The Duda and mid-crack perimeters were similar to that of the Freeman method if we assume that the radius is  $R+0.5$ .

Combining the estimators, the circularities are shown in the lower panel. Kulpa's perimeter and Gray's area gave the best result, close to but slightly larger than the true value of 1 for this test object. It is better than combining Kulpa's perimeter with Duda's area, although Duda's area is better than Gray's area. This is because Kulpa's perimeter and Gray's area are both slightly underestimated. Other combinations do not give good results, e.g. the mid-crack method.

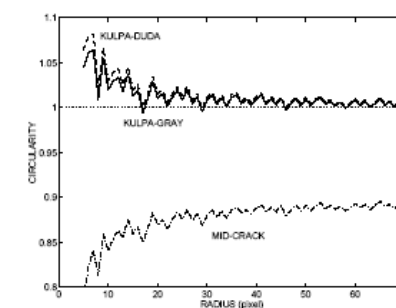
We note that the errors and the variability of the errors are largest when the value of  $R$  is small. We also note that the best results using two parameters (Gray's area and Kulpa's perimeter) that cannot be computed simultaneously. But Gray's area can be computed using a discrete Green's theorem, suggesting that the two estimators can be computed simultaneously during contour following.



(a)



(b)



## 1.2 Euler number – a topological feature

Topological shape features are a group of integer features that are invariant to scaling, rotation and even warping of the image. Warping can be visualized as the stretching of a rubber sheet containing the image of the object, to produce a spatially distorted object. Mappings that require cutting or pasting parts of the object are not allowed. Metric distances are clearly not topological features, nor features based on measuring angles.

However, connectivity is a topological feature, so the number of connected components in an image and the number of holes in objects are both topological features.

Bit quad counting provides a simple tool to determine the Euler number of a binary image. Under the assumption of four- and eight-connectivity, respectively, the Euler number is given by

$$E_4 = \frac{1}{4} [n\{Q_1\} - n\{Q_3\} + 2n\{Q_D\}]$$

$$E_8 = \frac{1}{4} [n\{Q_2\} - n\{Q_3\} - 2n\{Q_D\}]$$

It should be noted that while it is possible to compute the Euler number  $E$  of an image by such local neighborhood computations, neither the number of components  $C$  nor the number of holes  $H$  that make up  $E = C - H$  can be computed separately by local neighborhood computations.

## 2 Statistical moments

The general form of a moment of order  $(p+q)$ , evaluated over the complete image plane  $\xi$  is:

$$m_{pq} = \iint_{\xi} \psi_{pq}(x, y) f(x, y)$$

Where the weighting kernel or basis function is  $\psi_{pq}$ .

This produces a weighted description of the image  $f(x,y)$  integrated over the image plane  $\xi$ .

The basis functions may have a range of useful properties that are passed onto the moments, producing descriptions which can be invariant under rotation, scale, translation and orientation. To apply this to digital images, the equation above needs to be expressed in discrete form.

For simplicity we assume that  $\xi$  is divided into square pixels of dimension  $1 \times 1$ , with constant intensity  $I$  over each square pixel. The value of  $I$  is usually non-negative, and quantized to integer values from 0 to  $G-1$ , where  $G$  is the number of graylevels in the image.

So if  $P_{x,y}$  is a discrete pixel value then:

$$P_{xy} = I(x, y)\Delta A$$

where  $\Delta A$  is the sample or pixel area equal to one.

Thus,

$$M_{xy} = \sum_x \sum_y \psi(x, y) P(x, y); \quad p, q = 0, 1, 2, \dots, \infty$$

The choice of basis function depends on the application and on any desired invariant properties.

### 3 Non-orthogonal moments

The continuous two-dimensional  $(p + q)$ -th order Cartesian moment is defined as:

$$m_{pq} = \int_{-\infty}^{\infty} \int_{-\infty}^{\infty} x^p y^q f(x, y) dx dy$$

It is assumed that  $f(x, y)$  is a piecewise continuous, bounded function and that it can have non-zero values only in the finite region of the  $xy$  plane.

Then, moments of all orders exist and the uniqueness theorem holds:

***The moment sequence  $m_{pq}$  with basis  $x^p y^q$  is uniquely defined by  $f(x, y)$ ; and  $f(x, y)$  is uniquely defined by the moment sequence  $m_{pq}$ .***

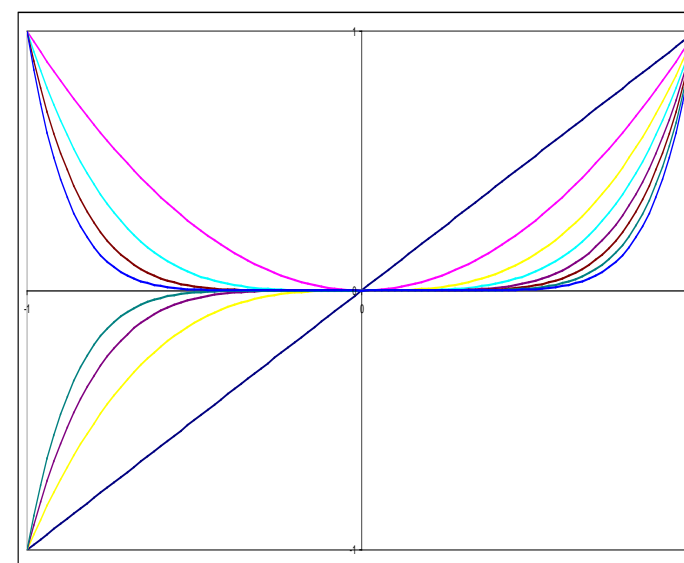
Thus, the original image can be described and reconstructed, provided that sufficiently high order moments are used.

The discrete version of the Cartesian moment for an image consisting of pixels  $P_{xy}$ , replacing the integrals with summations, is:

$$m_{pq} = \sum_{x=0}^{M-1} \sum_{y=0}^{N-1} x^p y^q P(x, y)$$

$m_{pq}$  is a two dimensional Cartesian moment, where  $M$  and  $N$  are the image dimensions and the monomial product  $x^p y^q$  is the basis function.

The figure to the right illustrates the first eight of these monomials for  $-1 < x < 1$ . We notice that for the positive  $X$ -axis, these monomials are highly correlated, which implies that we are going to need more moments to describe an object than if the basis functions were uncorrelated.



### 3.1 Low order Cartesian moments

The zero order moment  $m_{00}$  is defined as the total mass (or power) of the image.

$$m_{00} = \sum_{x=0}^{M-1} \sum_{y=0}^{N-1} f(x, y)$$

If this is applied to a binary  $M \times N$  image of an object, then this is simply a count of the number of pixels comprising the object, giving its area in pixels.

The two first order moments are used to find the Centre Of Mass (COM) of an image.

$$m_{10} = \sum_{x=0}^{M-1} \sum_{y=0}^{N-1} x f(x, y)$$

$$m_{01} = \sum_{x=0}^{M-1} \sum_{y=0}^{N-1} y f(x, y)$$

$$\bar{x} = \frac{m_{10}}{m_{00}}, \quad \bar{y} = \frac{m_{01}}{m_{00}}$$

If this is applied to a binary image, the expression is the same, but the computation is simpler, since the values of  $f(x,y)$  is binary: 0 or 1.

We will shortly see that these coordinates of the center of mass are useful to compute the central moments of an image.

## 3.2 Central moments

The 2D discrete central moment of an object is defined by a summation of the pixel values within a  $M \cdot N$  area covering the object:

$$\mu_{pq} = \sum_{x=0}^{M-1} \sum_{y=0}^{N-1} (x - \bar{x})^p (y - \bar{y})^q f(x, y)$$
$$\bar{x} = \frac{m_{10}}{m_{00}}, \quad \bar{y} = \frac{m_{01}}{m_{00}}$$

This is essentially a translated Cartesian moment, i.e., it corresponds to computing ordinary Cartesian moments after translating the object so that its center of mass coincides with the origin of the coordinate system.

This means that the central moments are invariant under translation.

However, central moments are not scaling or rotation invariant.

### 3.3 Computing central moments from ordinary moments

The 2D central moments  $\mu_{pq}$  can easily be computed from the ordinary moments  $m_{pq}$ .

A translation of an image  $f(x,y)$  by  $(\Delta x, \Delta y)$  in the  $(x,y)$ -direction gives a new image

$$f'(x, y) = f(x - \Delta x, y - \Delta y)$$

If we assume that we translate by an amount equal to the coordinates of the centre of mass;  $\Delta x = m_{10}/m_{00}$  and  $\Delta y = m_{01}/m_{00}$ , then the new moments of order  $p+q \leq 3$  are given by:

$$\begin{aligned}\mu_{00} &= m_{00} \\ \mu_{10} &= 0 \\ \mu_{01} &= 0 \\ \mu_{20} &= m_{20} - \bar{x}m_{10} \\ \mu_{02} &= m_{02} - \bar{y}m_{01} \\ \mu_{11} &= m_{11} - \bar{y}m_{10} \\ \mu_{30} &= m_{30} - 3\bar{x}m_{20} + 2\bar{x}^2m_{10} \\ \mu_{12} &= m_{12} - 2\bar{y}m_{11} - \bar{x}m_{02} + 2\bar{y}^2m_{10} \\ \mu_{21} &= m_{21} - 2\bar{x}m_{11} - \bar{y}m_{20} + 2\bar{x}^2m_{01} \\ \mu_{03} &= m_{03} - 3\bar{x}m_{02} + 2\bar{y}^2m_{01}\end{aligned}$$

The general 3D central moments  $\mu_{pqr}$  are generally expressed by the  $m_{pqr}$  moments:

$$\mu_{pqr} = \sum_{s=0}^p \sum_{t=0}^q \sum_{u=0}^r -1^{[D-d]} \binom{p}{s} \binom{q}{t} \binom{r}{u} \Delta x^{p-s} \Delta y^{q-t} \Delta z^{r-u} m_{stu}$$

Where  $D = (p + q + r)$ ,  $d = (s + t + u)$ , and the binomial coefficients are given by

$$\binom{v}{w} = \frac{v!}{w! (v-w)!}, \quad w < v$$

### 3.4 Second order central moments - moments of inertia

The two second order central moments of a 2D object are defined by

$$\mu_{20} = \sum_{x=0}^{M-1} \sum_{y=0}^{N-1} (x - \bar{x})^2 f(x, y)$$

$$\mu_{02} = \sum_{x=0}^{M-1} \sum_{y=0}^{N-1} (y - \bar{y})^2 f(x, y)$$

$$\bar{x} = \frac{m_{10}}{m_{00}}, \quad \bar{y} = \frac{m_{01}}{m_{00}}$$

and correspond to the “moments of inertia” relative to the coordinate directions, while the “cross moment of inertia” is given by

$$\mu_{11} = \sum_{x=0}^{M-1} \sum_{y=0}^{N-1} (x - \bar{x})(y - \bar{y})f(x, y)$$

The physical interpretation of a moment of inertia  $I$  of an object around a given axis is related to the kinetic energy in a rotational motion of the object around that particular axis. When a rigid body rotates about a fixed axis, the speed at a perpendicular distance  $r$  from the axis is  $v = r \omega$ , where  $\omega$  is the angular speed of the body. Now the rotational kinetic energy of the body is given by:

$$K = \frac{1}{2} I \omega^2$$

### 3.4.1 The parallel-axis theorem

A 2D or 3D object does not have just one moment of inertia. It has infinitely many, as there are an infinite number of axes about which it might rotate. But there is a simple relationship between the moment of inertia  $I_c$  of an object of mass  $M$  about an axis through its center of mass and the moment of inertia  $I_p$  about any other axis parallel to the original one but displaced from it by a distance  $d$ . This relationship is called the “parallel-axis theorem”, and simply states that

$$I_p = I_c + Md^2$$

To prove this, consider the figure to the right: We have

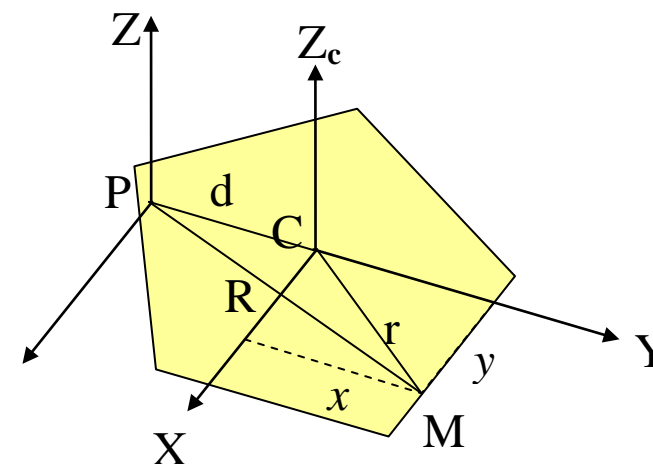
$$R^2 = r^2 + 2yd + d^2$$

The moment of inertia about the  $Z$ -axis is given by

$$\begin{aligned} I_p &= \sum mR^2 = \sum m(r^2 + 2yd + d^2) \\ &= \sum mr^2 + 2d \sum my + d^2 \sum m \\ &= I_c + 2dM\bar{y} + Md^2 \end{aligned}$$

But since the  $Z_c$ -axis is placed in the center of mass, the mean value of  $y$  is zero, so

$$I_p = I_c + Md^2$$



### 3.4.2 Moments of inertia of some regular 2D objects in the continuous case

#### 3.4.2.1 A rectangular object

Given a homogeneous (binary) rectangular object of size  $2a \cdot 2b$ , the moment of inertia around the y-axis is found by integrating the product of the length  $y$  of the black line and its distance  $x$  from the Y-axis. Since we have symmetry around the x-axis, the inertial moment is twice the integral above the X-axis:

$$I_{20} = 2 \int_{-a}^a x^2 b dx = 2b \left[ \frac{x^3}{3} \right]_{-a}^a = 2b \left[ \frac{a^3}{3} + \frac{a^3}{3} \right] = \underline{\underline{\frac{4}{3} a^3 b}}$$

Similarly, the moment of inertia around the X-axis is:

$$I_{02} = 2 \int_{-b}^b y^2 a dx = 2a \left[ \frac{y^3}{3} \right]_{-b}^b = 2a \left[ \frac{b^3}{3} + \frac{b^3}{3} \right] = \underline{\underline{\frac{4}{3} a b^3}}$$

Obviously, if the size of the rectangle is given as  $a \cdot b$ , the moments are  $a^3 b / 12$  and  $a b^3 / 12$ , respectively.

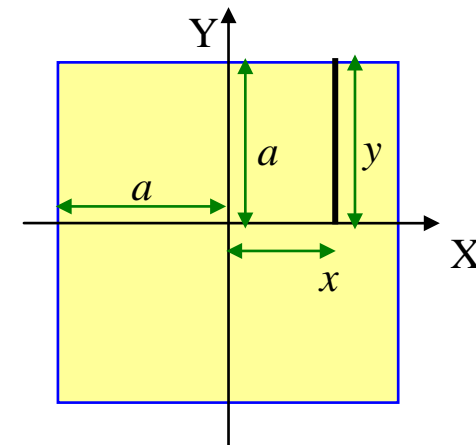
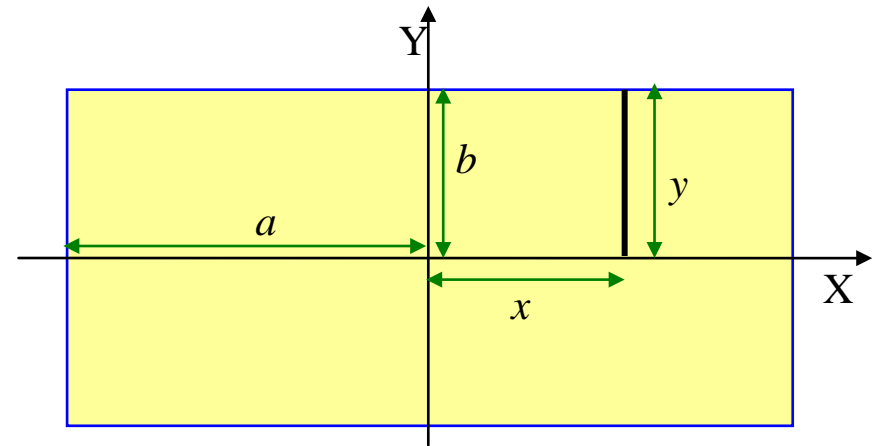
#### 3.4.2.2 A square object

For a homogeneous (binary) square object of size  $2a \cdot 2a$ , the moments of inertia around the X- and Y-axes are equal:

$$I_{20} = I_{02} = 2 \int_{-a}^a x^2 a dx = \underline{\underline{\frac{4}{3} a^4}}$$

And if the size of the square is given as  $a \cdot a$ , the moments are:

$$I_{20} = I_{02} = 2 \int_{-a/2}^{a/2} x^2 \frac{a}{2} dx = a \left[ \frac{x^3}{3} \right]_{-a/2}^{a/2} = a \left[ \frac{a^3}{24} + \frac{a^3}{24} \right] = \underline{\underline{\frac{1}{12} a^4}}$$



### 3.4.2.3 An elliptical object

For a homogeneous (binary) ellipse where the perimeter is given by

$$\left(\frac{x}{a}\right)^2 + \left(\frac{y}{b}\right)^2 = 1$$

we see that

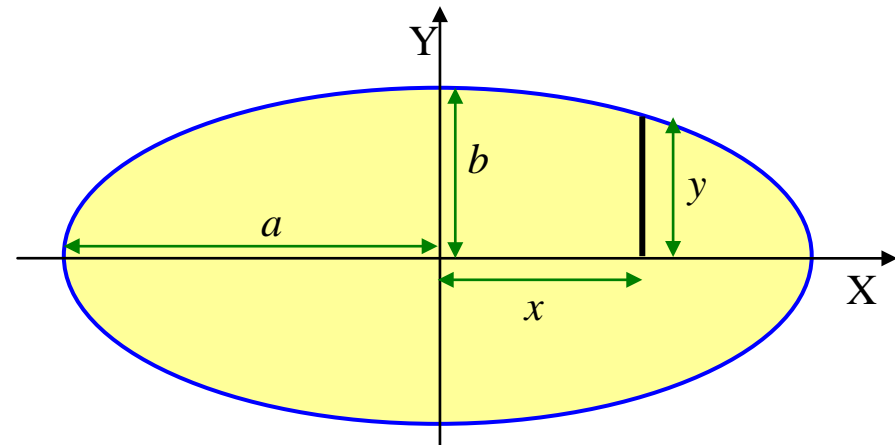
$$y = \pm \frac{b}{a} \sqrt{a^2 - x^2}$$

So the largest moment of inertia, that around the Y-axis, is found by integrating the product of the length  $y$  of the black line and its distance  $x$  from the Y-axis. Since we have symmetry around the x-axis, the inertial moment is twice the integral above the X-axis:

$$\begin{aligned} I_{20} &= 2 \frac{b}{a} \int_{-a}^a x^2 \sqrt{a^2 - x^2} dx \\ &= 2 \frac{b}{a} \left[ \frac{x}{8} (2x^2 - a^2) \sqrt{a^2 - x^2} + \frac{a^4}{8} \sin^{-1} \left( \frac{x}{a} \right) \right]_{-a}^a \\ &= 2 \frac{b}{a} \left[ \frac{a^4}{8} \left( \frac{\pi}{2} + \frac{\pi}{2} \right) \right] = \underline{\underline{\frac{\pi}{4} a^3 b}} \end{aligned}$$

Similarly, the smallest moment of inertia of the ellipse is given by

$$\begin{aligned} I_{02} &= 2 \frac{a}{b} \int_{-b}^b y^2 \sqrt{b^2 - y^2} dy \\ &= 2 \frac{a}{b} \left[ \frac{y}{8} (2y^2 - b^2) \sqrt{b^2 - y^2} + \frac{b^4}{8} \sin^{-1} \left( \frac{y}{b} \right) \right]_{-b}^b \\ &= 2 \frac{a}{b} \left[ \frac{b^4}{8} \left( \frac{\pi}{2} + \frac{\pi}{2} \right) \right] = \underline{\underline{\frac{\pi}{4} ab^3}} \end{aligned}$$



### 3.4.2.4 A circular object

For a homogeneous (binary) circular object where the perimeter is given by

$$x^2 + y^2 = R$$

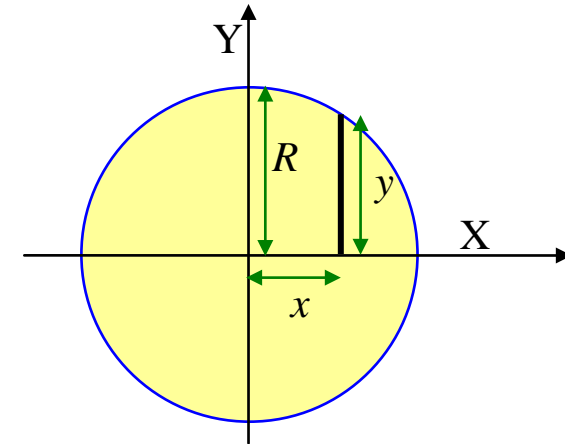
$$\Rightarrow y = \pm \sqrt{R^2 - x^2}$$

We see that the moments of inertia around the X- and Y-axes are now equal:

$$I_{20} = I_{02} = 2 \int_{-R}^R x^2 \sqrt{R^2 - x^2} dx$$

$$= 2 \left[ \frac{x}{8} (2x^2 - R^2) \sqrt{R^2 - x^2} + \frac{R^4}{8} \sin^{-1} \left( \frac{x}{R} \right) \right]_{-R}^R$$

$$= 2 \left[ \frac{R^4}{8} \left( \frac{\pi}{2} + \frac{\pi}{2} \right) \right] = \underline{\underline{\frac{\pi}{4} R^4}}$$



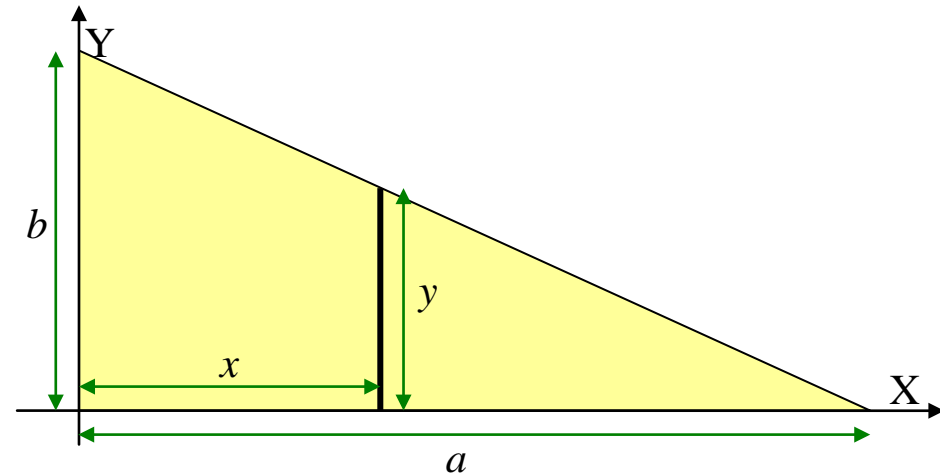
Obviously, we could arrive at the same expression from the moment of inertia of the elliptical object, setting  $a = b = R$ .

In fact, this is the moment of inertia of a binary circular object around any axis that lies in the XY-plane and that passes through the centre of the object.

### 3.4.2.5 A triangular object

Consider the homogeneous (binary) right angled triangle of size  $a \cdot b$  to the right. The coordinates of its center of mass are given by

$$\begin{aligned}\bar{x} &= \frac{m_{10}}{m_{00}} = \frac{2}{ab} \int_0^a xy \, dx = \frac{2}{ab} \int_0^a \left( bx - \frac{b}{a} x^2 \right) dx \\ &= \frac{2}{ab} \left[ \frac{b}{2} x^2 - \frac{b}{3a} x^3 \right]_0^a = \frac{2}{ab} \left[ \frac{a^2 b}{2} - \frac{a^3 b}{3a} \right] = \frac{a}{3}, \\ \bar{y} &= \frac{m_{01}}{m_{00}} = \frac{b}{3}\end{aligned}$$



Computing ordinary second order moments of this triangle, we find:

$$m_{20} = \int \int x^2 y \, dx = \int_0^a x^2 \left( b - \frac{b}{a} x \right) dx = \int_0^a \left( bx^2 - \frac{b}{a} x^3 \right) dx = \left[ \frac{b}{3} x^3 - \frac{b}{4a} x^4 \right]_0^a = \frac{a^3 b}{3} - \frac{a^4 b}{4a} = \frac{1}{12} a^3 b, \quad m_{02} = \frac{1}{12} ab^3$$

And we know how to compute central moments from ordinary moments:

$$\mu_{20} = m_{20} - \bar{x}m_{10}, \quad \mu_{02} = m_{02} - \bar{y}m_{01}$$

Where

$$\bar{x} = \frac{m_{10}}{m_{00}} \Rightarrow \bar{x}m_{10} = \bar{x}^2 m_{00}, \quad \bar{y} = \frac{m_{01}}{m_{00}} \Rightarrow \bar{y}m_{01} = \bar{y}^2 m_{00}$$

Thus, the moments of inertia of this triangular object around the x- and y-axis through its center of mass are given by

$$\mu_{20} = m_{20} - \bar{x}m_{10} = \frac{1}{12} a^3 b - \left( \frac{a}{3} \right)^2 \frac{ab}{2} = \frac{a^3 b}{12} - \frac{a^3 b}{18} = \frac{a^3 b}{36}, \quad \mu_{02} = \frac{ab^3}{36}$$

### 3.5 Perpendicular-axis theorem

Let us consider a homogeneous 2D object in the XY-plane, and let the origin O of the coordinate system be located at any point within or outside the object. Let  $I_X$  and  $I_Y$  be the moments of inertia about the X- and Y-axes and let  $I_Z$  be the moment of inertia about the Z-axis through O perpendicular to the XY-plane.

Considering an arbitrary point P within the object, we realize that the moment of inertia of this 2D object around the Z-axis is given by

$$I_Z = \int_{\text{object}} r^2 dr = \int_{\text{object}} (x^2 + y^2) dr = \int_{\text{object}} x^2 dr + \int_{\text{object}} y^2 dr$$

Noting that the moments of inertia relative to the X- and Y-axes are

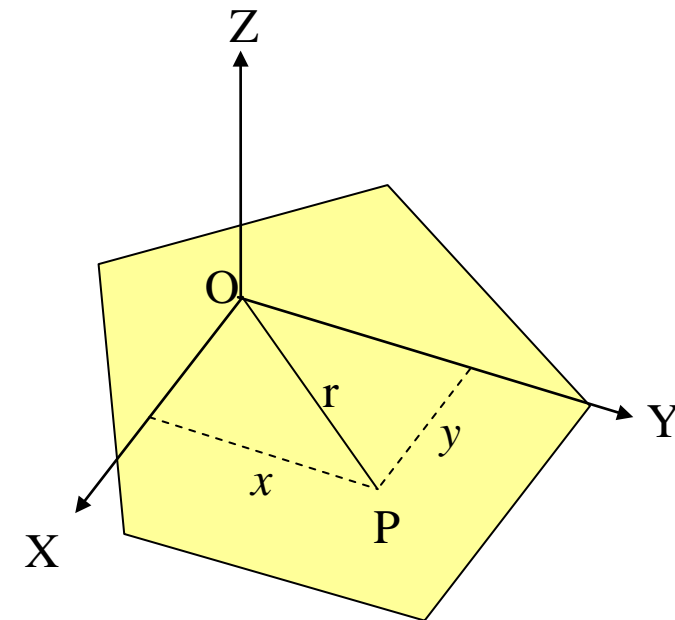
$$I_X = \int_{\text{object}} x^2 dr, \quad I_Y = \int_{\text{object}} y^2 dr$$

We realize that there is a very simple relation between the two orthogonal moments of inertia in the plane and the moment of inertia around an axis perpendicular to the plane through the crossing of the two orthogonal axes, namely

$$I_Z = I_X + I_Y$$

This is known as the “perpendicular-axis theorem”. For 3D objects it is only valid for thin plates in the XY-plane. Note that the origin of the coordinate system does not have to coincide with the center of mass of the object.

For a square object with side L, the moments of inertia around the X- and Y-axis passing through the center of the object are equal,  $I_X = I_Y = L^4/12$ . Thus, the moment of inertia around the Z-axis passing through the center of the object is  $I_Z = L^4/6$ . Obviously, the moment of inertia around the Z-axis must be independent of a rotation of the X- and Y-axis in the object plane. Therefore, we may conclude that the moment of inertia about ANY axis in the plane that passes through the center of a square is  $L^4/12$ .

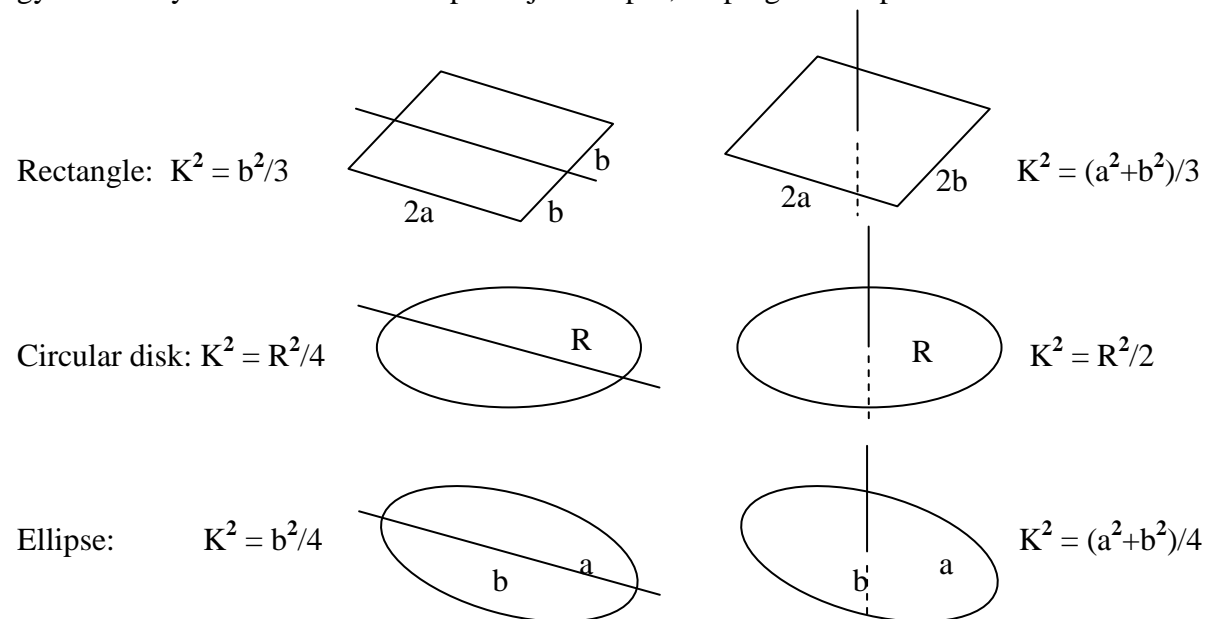


### 3.6 The radius of gyration

The radius of gyration  $K$  of an object is defined as the radius of a circle where we could concentrate all the mass of an object without altering the moment of inertia about its center of mass. So for an arbitrary object having a mass  $\mu_{00}$  and a moment of inertia around the  $Z$ -axis, we may write

$$I = \mu_{00} \hat{K}^2 \Rightarrow \hat{K} = \sqrt{\frac{I_Z}{\mu_{00}}} = \sqrt{\frac{I_X + I_Y}{\mu_{00}}} = \sqrt{\frac{\mu_{20} + \mu_{02}}{\mu_{00}}}$$

Obviously, this feature is invariant to rotation. It is a very useful quantity because it can be determined, for homogeneous objects, entirely by their geometry. Thus, the squared radius of gyration may be tabulated for simple object shapes, helping us compute the moments of inertia:



### 3.6.1.1 Examples: Three cylindrical objects

For a thin-walled hollow cylinder of radius  $R$  and height  $h$ , having a mass  $M = 2\pi Rh$ , the moment of inertia around its symmetry axis will be

$$I = r^2 2\pi rh = \underline{\underline{MR^2}}$$

Given a homogeneous cylindrical object of radius  $R$  and height  $h$ , the moment of inertia around its symmetry axis is found by integrating the product of the mass of a thin-walled hollow cylinder times the square of its radius, from the z-axis out to the radius  $R$  of the cylinder.

Utilizing the fact that the mass of this cylinder is  $M = \pi R^2 h$ , we get:

$$I = \int_0^R r^2 2\pi rh \, dr = 2\pi h \left[ \frac{r^4}{4} \right]_0^R = \frac{1}{2} \pi R^4 h = \underline{\underline{\frac{1}{2} MR^2}}$$

If the cylinder is hollow, with an inner radius  $R_1$  and an outer radius  $R_2$ , its mass  $M$  and its moment of inertia around the symmetry axis are given by

$$M = \pi h (R_2^2 - R_1^2)$$

$$I = \int_{R_1}^{R_2} r^2 2\pi rh \, dr = 2\pi h \left[ \frac{r^4}{4} \right]_{R_1}^{R_2} = \frac{1}{2} \pi h [R_2^4 - R_1^4] = \frac{1}{2} \pi h (R_2^2 - R_1^2)(R_2^2 + R_1^2) = \underline{\underline{\frac{1}{2} M (R_2^2 + R_1^2)}}$$

### 3.6.1.2 From solid cylinder to solid sphere

We have seen that the moment of inertia of a disk of radius  $r$  and mass  $dm$  around its symmetry axis is  $r^2 dm/2$ .

If we divide a sphere into thin disks, the radius of the disk at a distance  $x$  from the center of the sphere is

$$r = \sqrt{R^2 - x^2}$$

Its mass is proportional to its area

$$dm = \pi(R^2 - x^2)$$

So the moment of inertia of a thin slice of a sphere is

$$dI = \frac{1}{2} r^2 dm = \frac{1}{2} (\sqrt{R^2 - x^2})^2 [\pi(R^2 - x^2)]$$

Integrating this expression from  $x = 0$  to  $x = R$  gives the moment of inertia of the right hand hemisphere. The total moment of inertia of the whole sphere is just twice this:

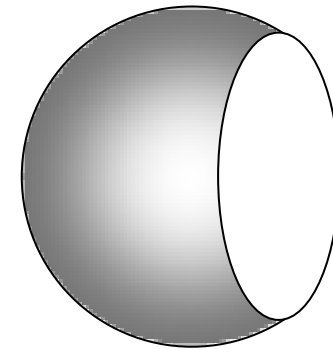
$$I = \pi \int_0^R (R^2 - x^2)^2 dx = \pi \int_0^R [R^4 - 2R^2 x^2 + x^4] dx = \pi \left[ R^4 x - \frac{2}{3} R^2 x^3 + \frac{1}{5} x^5 \right]_0^R = \frac{8\pi}{15} R^5$$

Now the mass of a homogeneous sphere of unit mass density is

$$M = \frac{4}{3} \pi R^3$$

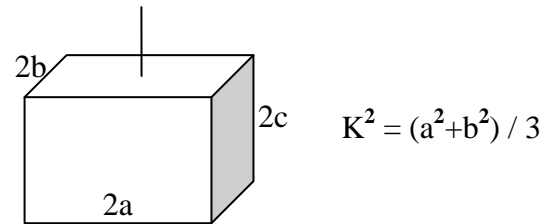
So the moment of inertia of a solid homogeneous sphere is simply:

$$I = \frac{2}{5} MR^2$$



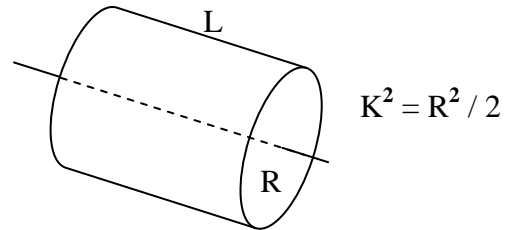
### 3.6.1.3 Radii of gyration of some homogenous solid objects

Solid parallelepiped:



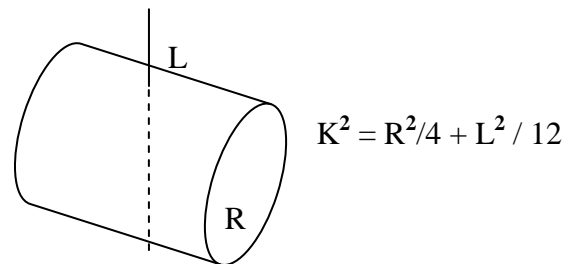
$$K^2 = (a^2 + b^2) / 3$$

Solid cylinder:



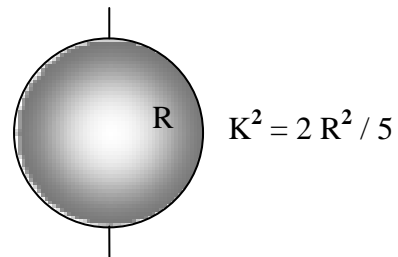
$$K^2 = R^2 / 2$$

Solid cylinder:



$$K^2 = R^2 / 4 + L^2 / 12$$

Solid sphere:



$$K^2 = 2 R^2 / 5$$

### 3.6.2 Estimating object orientation from inertial moments

The orientation of an object is defined as the angle, relative to the X-axis, of an axis through the centre of mass of the object that gives the lowest moment of inertia of the object relative to that axis.

Let us assume that we have a 2D object  $f(x,y)$ , and that the Cartesian X,Y-coordinates have their origin in the centre of mass of the object. We further assume that the object has a unique orientation, i.e., that there exists a rotated coordinate system  $(\alpha,\beta)$ , such that if we compute the moment of inertia of the object around the  $\alpha$ -axis, this will be the smallest possible moment of inertia for this particular object. In order to find the orientation  $\theta$  of this  $\alpha$  axis relative to the X-axis, we have to minimize the second order central moment of the object around the  $\alpha$ -axis:

$$I(\theta) = \sum_{\alpha} \sum_{\beta} \beta^2 f(\alpha, \beta)$$

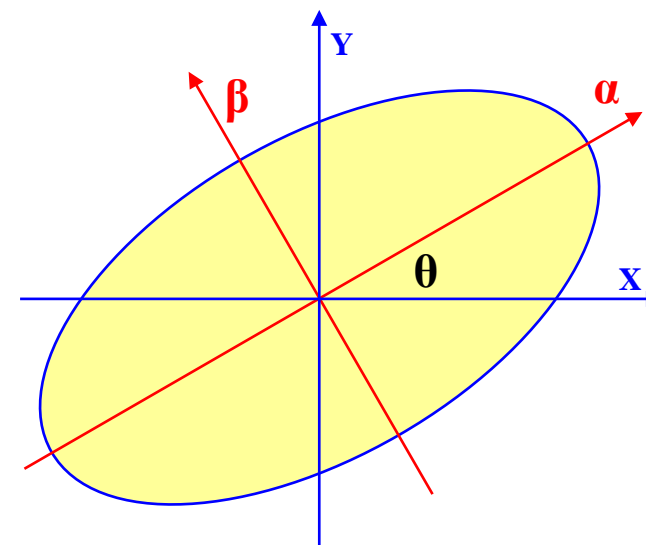
where the rotated coordinates are given by

$$\alpha = x \cos \theta + y \sin \theta, \quad \beta = -x \sin \theta + y \cos \theta$$

Then we get the second order central moment of the object around the  $\alpha$ -axis, expressed in terms of  $x, y$ , and the orientation angle  $\theta$  of the object:

$$I(\theta) = \sum_x \sum_y [y \cos \theta - x \sin \theta]^2 f(x, y)$$

Since we are looking for the minimum value of this moment of inertia, we take the derivative of this expression with respect to the angle  $\theta$ , set the derivative equal to zero, and see if we can find a simple expression for  $\theta$  :



$$\begin{aligned}
\frac{\partial}{\partial \theta} I(\theta) &= \sum_x \sum_y 2f(x, y) [y \cos \theta - x \sin \theta] [-y \sin \theta - x \cos \theta] = 0 \\
&\Downarrow \\
\sum_x \sum_y 2f(x, y) [xy (\cos^2 \theta - \sin^2 \theta)] &= \sum_x \sum_y 2f(x, y) [x^2 - y^2] \sin \theta \cos \theta \\
&\Downarrow \\
2\mu_{11} (\cos^2 \theta - \sin^2 \theta) &= 2(\mu_{20} - \mu_{02}) \sin \theta \cos \theta \\
\Box \Downarrow \\
\frac{2\mu_{11}}{(\mu_{20} - \mu_{02})} &= \frac{2 \sin \theta \cos \theta}{(\cos^2 \theta - \sin^2 \theta)} = \frac{2 \tan \theta}{1 - \tan^2 \theta} = \tan(2\theta)
\end{aligned}$$

So the object orientation is quite easily obtained from the three central moments of inertia:

$$\underline{\underline{\theta = \frac{1}{2} \tan^{-1} \left[ \frac{2\mu_{11}}{(\mu_{20} - \mu_{02})} \right]}}, \quad \text{where } \theta \in [0, \pi/2] \text{ if } \mu_{11} > 0, \quad \theta \in [\pi/2, \pi] \text{ if } \mu_{11} < 0$$

### 3.7 The best fitting object ellipse

The object ellipse is defined as the ellipse whose least and greatest moments of inertia equal those of the object. This is regarded as the ellipse that fits best to the object. Its size and eccentricity is invariant to orientation.

The semimajor and semiminor axes of this ellipse are given by

$$(\hat{a}, \hat{b}) = \sqrt{\frac{2 \left[ \mu_{20} + \mu_{02} \pm \sqrt{(\mu_{20} + \mu_{02})^2 + 4\mu_{11}^2} \right]}{\mu_{00}}}$$

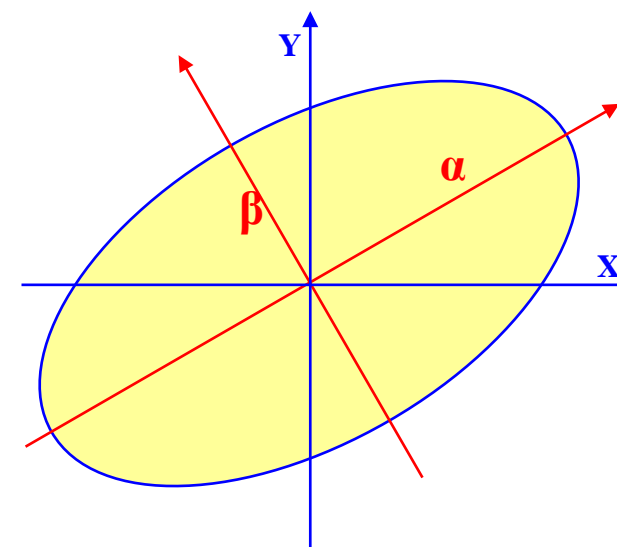
While the numerical eccentricity of the best fit ellipse is given by

$$\hat{\varepsilon} = \sqrt{\frac{\hat{a}^2 - \hat{b}^2}{\hat{a}^2}}$$

Notice that the numerical eccentricity is a bounded measure; it is 0 for a perfectly circular object, and goes asymptotically towards 1 the more elongated the object is; ( $0 \leq \varepsilon < 1$ ).

This is very different from the simplified “eccentricity of the bounding box”; ( $1 \leq e = a/b < \infty$ ).

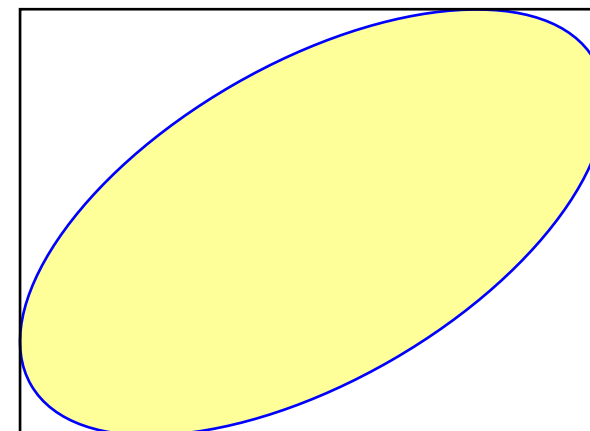
We also notice that all three orientation invariant object features above are computed from the three second order central moments of a 2D object (moments of inertia) and the total mass of the object, no matter whether it is a gray scale or binary object.



### 3.8 The bounding rectangles of an object

There are two kinds of bounding rectangles that we may place around a 2D object; the “image-oriented” and the “object-oriented” bounding rectangle. For 3D objects, this extends to “bounding-boxes”, although the term “box” is also often used in 2D images. We will illustrate these two concepts for a simple elliptical object to show that the size, shape, and orientation of the two types of bounding rectangle may be very different.

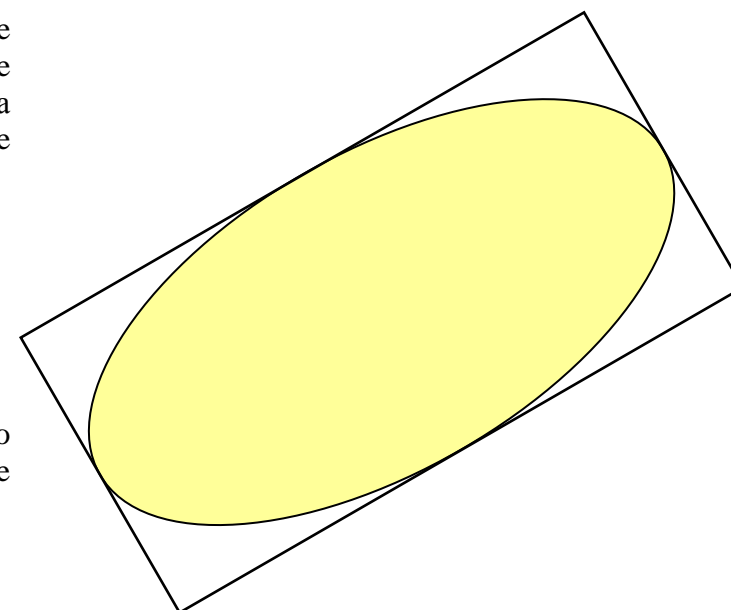
The “image-oriented” bounding rectangle is the smallest rectangle having sides that are parallel to the edges of the image that can be placed around the object. It is found by simply searching through the object (or rather its perimeter) for the minimum and maximum value of its X- and Y- coordinates. So it is simply represented by the coordinates of two opposite corners: e.g.  $(x_{\min}, y_{\min})$  and  $(x_{\max}, y_{\max})$ , as illustrated in the figure to the right. Evidently, the size and elongation of this bounding box depends on the orientation of the object.



The “object-oriented” bounding rectangle is the smallest rectangle having its longest side parallel to the orientation of the object that can be placed around the object. If we have estimated the orientation  $\theta$  of the object (see previous section), we may perform a transformation of all pixels along the perimeter of the object from the X,Y-coordinates of the image to a rotated Cartesian coordinate system  $\alpha, \beta$  by

$$\begin{aligned}\alpha &= x \cos \theta + y \sin \theta \\ \beta &= -x \sin \theta + y \cos \theta\end{aligned}$$

Then we search for the minimum and maximum value of its  $\alpha$  and  $\beta$  coordinates. So the “object oriented” bounding rectangle is simply represented by the coordinates of two opposite corners in the  $\alpha, \beta$ -domain: e.g.  $(\alpha_{\min}, \beta_{\min})$  and  $(\alpha_{\max}, \beta_{\max})$ , as illustrated in the figure to the right. Obviously, the size and shape of this bounding box is invariant to rotation.



### 3.9 Scaling invariant central moments

If we transform an image by changing the scale of the image  $f(x,y)$  by  $\alpha$  in the X-direction and  $\beta$  in the Y-direction, we get a new image  $f'(x,y) = f(x/\alpha,y/\beta)$ .

The relation between a central moment  $\mu_{pq}$  in the original image and the corresponding central moment  $\mu'_{pq}$  in the transformed image is

$$\mu'_{pq} = \alpha^{1+p} \beta^{1+q} \mu_{pq}$$

For  $\beta = \alpha$  we have

$$\mu'_{pq} = \alpha^{2+p+q} \mu_{pq}$$

Thus, we get scaling invariant central moments by a simple normalization of the central moments:

$$\eta_{pq} = \frac{\mu_{pq}}{(\mu_{00})^\gamma}, \quad \gamma = \frac{p+q}{2} + 1, \quad \forall (p+q) \geq 2$$

### 3.10 Symmetry, skewness and kurtosis

A measure of asymmetry in an image is given by its *skewness*. The skewness is a statistical measure of a distribution's degree of deviation from symmetry about the mean. The degree of skewness in the x and y direction can be determined by the two third order central moments,  $\mu_{30}$  and  $\mu_{03}$ , respectively

Here symmetry is being detected about the center of mass of the image, hence the use of the central moments. In order to compare symmetry properties of objects regardless of scale, the first seven scale-normalised central moments ( $\eta_{11}$ ,  $\eta_{20}$ ,  $\eta_{02}$ ,  $\eta_{21}$ ,  $\eta_{12}$ ,  $\eta_{30}$ ,  $\eta_{03}$ ) may be used.

- Objects that are either symmetric about the x or y axes will produce  $\eta_{11} = 0$ .
- Objects with a strict symmetry about the y axis will give  $\eta_{12} = 0$  and  $\eta_{30} = 0$ .
- Objects with a strict symmetry about the x axis will give  $\eta_{21} = 0$  and  $\eta_{03} = 0$ .
  
- For shapes symmetric about the x axis,  $\eta_{pq} = 0$  for all  $p = 0, 2, 4, \dots$ ;  $q = 1, 3, 5, \dots$

The sign of the first seven scale normalised central moments ( $\eta_{11}$ ,  $\eta_{20}$ ,  $\eta_{02}$ ,  $\eta_{21}$ ,  $\eta_{12}$ ,  $\eta_{30}$ ,  $\eta_{03}$ ) may be tabulated for three different types of simple symmetry; symmetry about the Y-axis, symmetry about the X-axis, and symmetry about both the X- and Y-axis; exemplified by the printed capital characters M, C and O:

Character	$\eta_{11}$	$\eta_{20}$	$\eta_{02}$	$\eta_{21}$	$\eta_{12}$	$\eta_{30}$	$\eta_{03}$
<b>M</b>	<b>0</b>	+	+	-	<b>0</b>	<b>0</b>	-
<b>C</b>	<b>0</b>	+	+	<b>0</b>	+	+	<b>0</b>
<b>O</b>	<b>0</b>	+	+	<b>0</b>	<b>0</b>	<b>0</b>	<b>0</b>

### 3.10.1 Skewness

Skewness is the degree of asymmetry, or departure from symmetry, of a distribution.

If the frequency curve of a distribution has a longer tail to the right of the central maximum than to the left, the distribution is said to be skewed to the right, or to have a positive skewness. If the reverse is true, it is said to be skewed to the left, or to have a negative skewness.

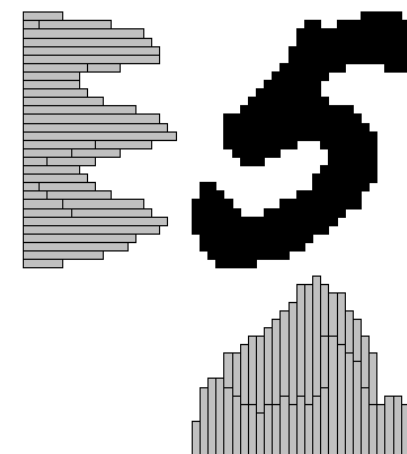
An important measure of skewness uses the third moment about the mean expressed in dimensionless form, given by

$$a_3 = \frac{\mu_{30}}{\sigma^3} = \frac{\sqrt{n} \sum_{i=1}^n (x_i - \bar{x})^3}{\left( \sum_{i=1}^n (x_i - \bar{x})^2 \right)^{3/2}}$$

For perfectly symmetrical distributions,  $a_3$  is zero.

For skewed distributions, the mean and the median tend to lie on the same side of the mode as the longer tail. Thus, a simple measure of the asymmetry is the differences (mean – mode), which can be made dimensionless if divided by a measure of dispersion, such as the standard deviation (Pearson's first coefficient of skewness). An alternative is to use the median instead of the mode (Pearson's second coefficient of skewness).

It may be tempting to test for symmetry and skewness using the two 1D projection histograms of a 2D binary object. Similarity measures based on comparison of cumulative projection histograms may be useful at various stages of OCR systems. But as illustrated by the figure to the right, a 1D projection histogram may appear almost symmetric, even though the projection is not performed in the direction of the orientation of the 2D object. It is also obvious that if a e.g. S-shaped, point-symmetric object is projected in the directions of its principal axes, the 1D projection histograms will be consistent with axial symmetry, although that does not exist.



### 3.10.2 Kurtosis

If the object is symmetric around an axis having a certain orientation, it may be of interest to quantify the distribution of the distance of the object elements from the symmetry axis, compared to the normal distribution of the same variance. This may be done using the statistical kurtosis.

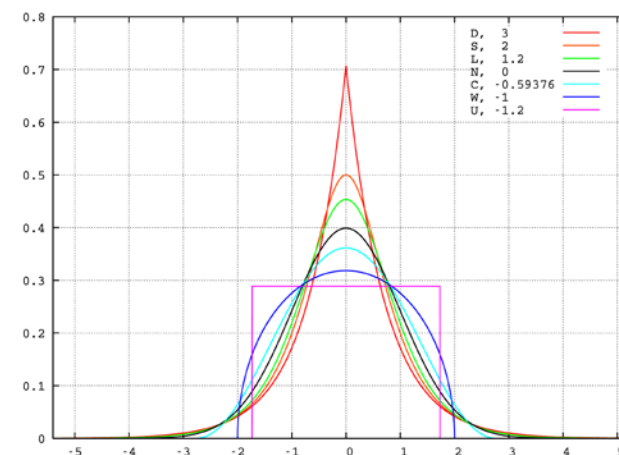
Kurtosis is defined by the fourth moment normalized by the square of the variance. The constant 3 is subtracted in order to make the kurtosis of the normal distribution equal to zero. Higher kurtosis means that more of the variance is due to infrequent extreme x-values.

Kurtosis is being detected about the center of mass of the image, so we use of the central moments. First the orientation of the object is found and the object is rotated, so that its principal axis coincides with the Y-axis of the coordinate system. Then, the kurtosis is given by:

$$a_4 = \frac{\mu_{40}}{\mu_{20}^2} - 3 = \frac{n \sum_{i=1}^n (x_i - \bar{x})^4}{\left( \sum_{i=1}^n (x - \bar{x})^2 \right)^2} - 3$$

We may project a 2D binary object onto its principal axes. Assuming that the resulting 1D projection histograms are considered to be unimodal and symmetric, we may use the kurtosis of the distributions to distinguish between different shapes, since the kurtosis of parametric distributions are well known:

- Uniform (U), kurtosis = -1.2
- Semicircular (W), kurtosis = -1
- Raised Cosine (C), kurtosis = -0,6
- Normal (N), kurtosis = 0
- Logistic (L), kurtosis = 1.2
- Hyperbolic secant, (S), kurtosis = 2
- Laplace (D), kurtosis = 3



### 3.11 Hu's invariant set of moments

Hu (1962) described two different methods for producing rotation invariant moments.

The first requires finding the principal axes of the object, and then computing the scale normalized central moments of a rotated object. However, this method can break down when images do not have unique principal axes. Such images are described as being rotationally symmetric.

The second method described by Hu utilizes nonlinear combinations of scale normalized central moments that are useful for scale, position, and rotation invariant pattern identification. A set of seven such invariants is often used.

For second order moments ( $p+q=2$ ), two invariants are used:

$$\varphi_1 = \eta_{20} + \eta_{02} \quad \varphi_2 = (\eta_{20} - \eta_{02})^2 + 4\eta_{11}^2$$

For third order moments, ( $p+q=3$ ), the invariants are:

$$\varphi_3 = (\eta_{30} - 3\eta_{12})^2 + (3\eta_{21} - \eta_{03})^2$$

$$\varphi_4 = (\eta_{30} + \eta_{12})^2 + (\eta_{21} + \eta_{03})^2$$

$$\varphi_5 = (\eta_{30} - 3\eta_{12})(\eta_{30} + \eta_{12})[(\eta_{30} + \eta_{12})^2 - 3(\eta_{21} + \eta_{03})^2] + (3\eta_{21} - \eta_{03})(\eta_{21} + \eta_{03})[3(\eta_{30} + \eta_{12})^2 - (\eta_{21} + \eta_{03})^2]$$

$$\varphi_6 = (\eta_{20} - \eta_{02})[(\eta_{30} + \eta_{12})^2 - (\eta_{21} + \eta_{03})^2] + 4\eta_{11}(\eta_{30} + \eta_{12})(\eta_{21} + \eta_{03})$$

$$\varphi_7 = (3\eta_{21} - \eta_{03})(\eta_{30} + \eta_{12})[(\eta_{30} + \eta_{12})^2 - 3(\eta_{21} + \eta_{03})^2] - (\eta_{30} - 3\eta_{12})(\eta_{21} + \eta_{03})[3(\eta_{30} + \eta_{12})^2 - (\eta_{21} + \eta_{03})^2]$$

$\varphi_7$  is skew invariant, and may help distinguish between mirror images.

Using

$$\mathbf{a} = (\eta_{30} - 3\eta_{12}), \quad \mathbf{b} = (3\eta_{21} - \eta_{03}), \quad \mathbf{c} = (\eta_{30} + \eta_{12}), \quad \text{and} \quad \mathbf{d} = (\eta_{21} + \eta_{03})$$

we may simplify the five last invariants of the set:

$$\varphi_3 = \mathbf{a}^2 + \mathbf{b}^2$$

$$\varphi_4 = \mathbf{c}^2 + \mathbf{d}^2$$

$$\varphi_5 = \mathbf{ac}[\mathbf{c}^2 - 3\mathbf{d}^2] + \mathbf{bd}[3\mathbf{c}^2 - \mathbf{d}^2]$$

$$\varphi_6 = (\eta_{20} - \eta_{02})[\mathbf{c}^2 - \mathbf{d}^2] + 4\eta_{11}\mathbf{cd}$$

$$\varphi_7 = \mathbf{bc}[\mathbf{c}^2 - 3\mathbf{d}^2] - \mathbf{ad}[3\mathbf{c}^2 - \mathbf{d}^2]$$

These moments are of finite order, therefore, unlike the central moments they do not comprise a complete set of image descriptors. However, higher order invariants can be derived.

It should be noted that this method also breaks down, as with the method based on the principal axis for images which are rotationally symmetric as the seven invariant moments will be zero.

### 3.12 The Hu moments for simple symmetric 2D objects

The simplest elongated and symmetric objects are binary rectangles and ellipses.

In the continuous case, the two moments of inertia of a binary rectangular object of size  $2a$  by  $2b$ , having its major axis in the direction of the X-axis are given by

$$\mu_{20} = \frac{4}{3}a^3b, \quad \mu_{02} = \frac{4}{3}ab^3$$

The size of this object is  $4ab$ , and the scale and position invariant moments  $\eta_{20}$  and  $\eta_{02}$  are

$$\eta_{20} = \frac{1}{12} \frac{a}{b}, \quad \eta_{02} = \frac{1}{12} \frac{b}{a}$$

As we have seen, the four scale normalized moments ( $\eta_{11}$ ,  $\eta_{21}$ ,  $\eta_{12}$ ,  $\eta_{30}$ ,  $\eta_{03}$ ) are all zero for an object that is symmetric about both the X- and Y-axis. So the two first Hu moments are

$$\phi_1 = \frac{1}{12} \left( \frac{a}{b} + \frac{b}{a} \right), \quad \phi_2 = \left( \frac{1}{12} \right)^2 \left( \frac{a}{b} - \frac{b}{a} \right)^2$$

and the remaining five Hu moments are all zero.

Similarly, the two moments of inertia of a binary elliptic object with semi-axes  $a$  and  $b$ , having its major axis in the direction of the X-axis are given by

$$\mu_{20} = \frac{\pi}{4}a^3b, \quad \mu_{02} = \frac{\pi}{4}ab^3$$

The size of this object is  $\pi ab$ , and the scale and position invariant moments  $\eta_{20}$  and  $\eta_{02}$  are

$$\eta_{20} = \frac{1}{4\pi} \frac{a}{b}, \quad \eta_{02} = \frac{1}{4\pi} \frac{b}{a}$$

Again, the four scale normalized moments ( $\eta_{11}$ ,  $\eta_{21}$ ,  $\eta_{12}$ ,  $\eta_{30}$ ,  $\eta_{03}$ ) are all zero for such a symmetric object, and the two first Hu moments are simply

$$\phi_1 = \frac{1}{4\pi} \left( \frac{a}{b} + \frac{b}{a} \right), \quad \phi_2 = \left( \frac{1}{4\pi} \right)^2 \left( \frac{a}{b} - \frac{b}{a} \right)^2$$

while the remaining five Hu moments are all zero.

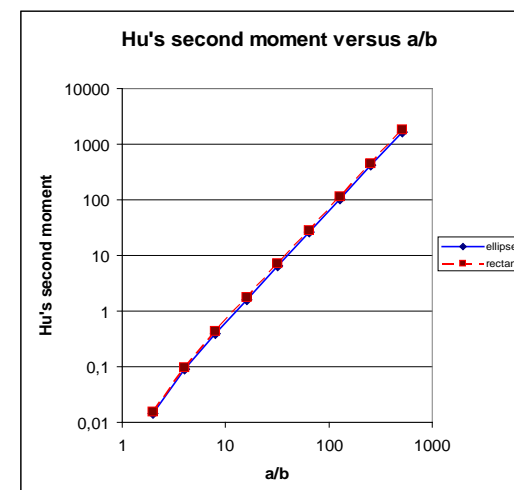
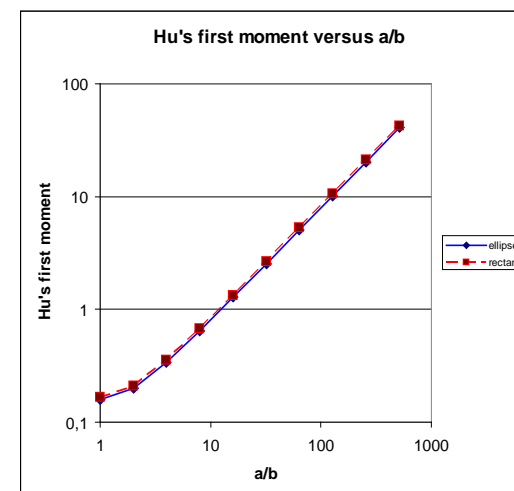
Thus, only the two second-order Hu moments ( $\phi_1$ ,  $\phi_2$ ) are useful for these simple objects.

In the logarithmic plots to the right, the first two Hu moments have been plotted versus  $a/b$  for 10 values of  $a/b$ :  $a = b$ ,  $a = 2b$ , ...,  $a = 512b$ . We notice that even in the continuous case it may be hard to distinguish between an ellipse and its bounding rectangle using these two moments.

In fact, the relative difference in the first Hu moments of an ellipse and its object oriented bounding rectangle is constant, 4.5%, regardless of the size and eccentricity of the ellipse.

Similarly, the relative difference in the second Hu moments of an ellipse and its object oriented bounding rectangle is also constant for all ellipses, 8.8%, except when the ellipse degenerates to a circle, for which  $\phi_2 = 0$ , both for the circle and its bounding square.

Since the Hu moments are scale invariant, they are unaltered if we shrink the object oriented bounding rectangle of an ellipse so that the rectangle has the same area as the ellipse, maintaining the  $a/b$  ratio. Thus, the relative differences given above are also true when comparing an ellipse with a same-area rectangle having the same  $a/b$  ratio, regardless of the size and eccentricity of the ellipse.



### 3.13 Relation to compactness for simple objects

Haralick and Shapiro (1993) defines "Roundness or compactness  $\gamma = P^2/(4\pi A)$ . For a disc,  $\gamma$  is minimum and equals 1. In the digital domain it takes its smallest value not for a circle but for a digital octagon or diamond, depending on whether 8-connectivity or 4-connectivity is used in calculating the perimeter."

This compactness measure  $\gamma$  attains a high value for objects where the square of the length of its perimeter is large as compared to its area. This happens for both complex objects, and for very elongated simple objects, like rectangles and ellipses where the  $a/b$  ratio is high.

For ellipses and rectangles, the compactness measure in the continuous case is given by:

$$\gamma_{\text{ellipse}} = \frac{1}{4} \left( \frac{a}{b} + \frac{b}{a} \right), \quad \gamma_{\text{rectangle}} = \frac{1}{\pi} \left( \frac{a}{b} + \frac{b}{a} + 2 \right)$$

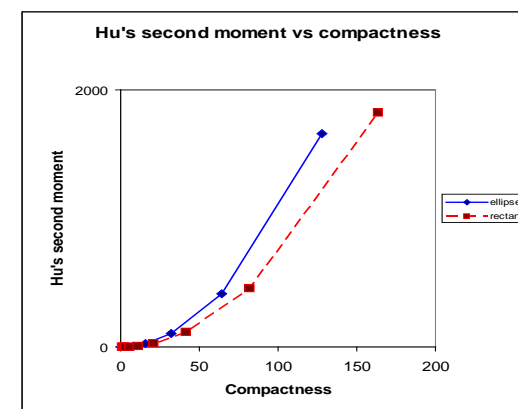
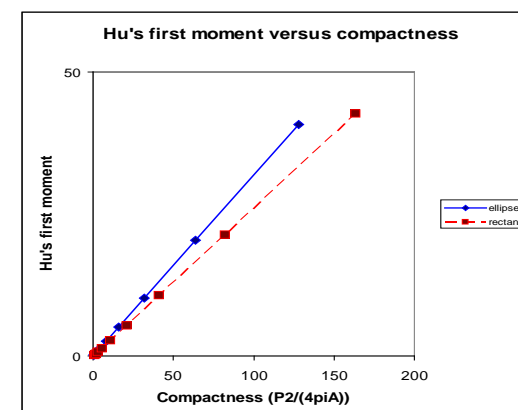
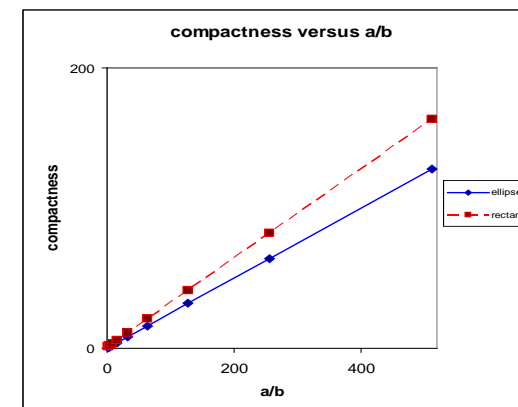
as illustrated in the linear plot to the right of the compactness measure as a function of the  $a/b$  ratio.

We notice that for ellipses, the first Hu moment is a simple linear function of its compactness measure, given by  $\phi_1 = \gamma/\pi$ , while for rectangles the relationship is a little more complicated, but still approximately linear:  $\phi_1 = \gamma (\pi/12)(a^2+b^2)/(a+b)^2$ , as illustrated in the linear plot to the right. Thus, using both the compactness measure and the first Hu moment to characterize ellipses or rectangles seems redundant, regardless of their size and elongation.

For ellipses and their object oriented bounding rectangles, the relationships between the second Hu moment and the compactness measure are nonlinear and depend on the  $a/b$  ratio. For an ellipse,  $\phi_2 = \gamma (1/4\pi^2 ab)(a^2-b^2)^2/(a^2+b^2)$ , and for the object oriented bounding rectangle the relationship is:  $\phi_2 = \gamma (\pi/144)(a/b - 1)(1 - b/a)$ , as illustrated in the linear plot below.

Thus, the second Hu moment seems to be a more valuable feature than the first Hu moment if the compactness measure is also used to characterize ellipses and rectangles.

We also note that if the object deviates from the simple symmetry of ellipses and rectangles, the second Hu moment is also sensitive to asymmetry, while this is not the case for the first Hu moment.



### 3.14 Affine invariants

Flusser and Suk (1993) give set of four moments are invariant under general affine transforms:

$$I_1 = \frac{\mu_{20}\mu_{02} - \mu_{11}^2}{\mu_{00}^4}$$

$$I_2 = \frac{\mu_{30}^2\mu_{03}^2 - 6\mu_{30}\mu_{21}\mu_{12}\mu_{03} + 4\mu_{30}\mu_{12}^3 + 4\mu_{21}^3\mu_{03} - 3\mu_{12}^2\mu_{21}^2}{\mu_{00}^{10}}$$

$$I_3 = \frac{\mu_{20}(\mu_{21}\mu_{30} - \mu_{12}^2) - \mu_{11}(\mu_{30}\mu_{03} - \mu_{21}\mu_{12}) + \mu_{02}(\mu_{30}\mu_{12} - \mu_{21}^2)}{\mu_{00}^7}$$

$$I_4 = (\mu_{20}^3\mu_{03}^2 - 6\mu_{20}^2\mu_{11}\mu_{12}\mu_{03} - 6\mu_{20}^2\mu_{02}\mu_{21}\mu_{03} + 9\mu_{20}^2\mu_{02}\mu_{12}^2 + 12\mu_{20}\mu_{11}^2\mu_{21}\mu_{03} \\ + 6\mu_{20}\mu_{11}\mu_{02}\mu_{30}\mu_{03} - 18\mu_{20}\mu_{11}\mu_{02}\mu_{21}\mu_{12} - 8\mu_{11}^2\mu_{30}\mu_{03} - 6\mu_{20}\mu_{02}^2\mu_{30}\mu_{12} \\ + 9\mu_{20}\mu_{11}^2\mu_{21}\mu_{03} + 12\mu_{20}\mu_{02}^2\mu_{21}^2 + 12\mu_{11}^2\mu_{02}\mu_{30}\mu_{12} - 6\mu_{11}\mu_{02}^2\mu_{21} + \mu_{02}^3\mu_{30}^2) / \mu_{00}^{11}$$

Flusser (2000) has given an excellent overview of the independence of rotation moment invariants.

### 3.15 Fast computation of moments

A huge effort has been put into finding effective algorithms for moment calculations. A review is given by Yang and Albrechtsen (1996). An often used algorithm for fast, but not exact computation of moments is given Li and Chen (1991). Faster and exact algorithms are given by Yang and Albrechtsen (1996) and Yang, Albrechtsen, and Taxt (1997).

### 3.16 Contrast invariants

A change in contrast gives a new intensity distribution  $f'(x, y) = cf(x, y)$ .

The transformed moments are then

$$\mu'_{pq} = c \mu_{pq}$$

Abo-Zaid *et al.* (1988) have defined a normalization that cancels both scaling and contrast.

The normalization is given by

$$\eta'_{pq} = \frac{\mu_{pq}}{\mu_{00}} \left( \frac{\mu_{00}}{\mu_{20} + \mu_{02}} \right)^{\frac{(p+q)}{2}}$$

If we use  $\mu'_{00} = c\alpha^2\mu_{00}$ ,  $\mu'_{02} = c\alpha^4\mu_{02}$ , and  $\mu_{20} = c\alpha^4\mu_{20}$ , we easily see that  $\eta'_{pq}$  is invariant to both scale and contrast.

This normalization also reduces the dynamic range of the moment features, so that we may use higher order moments without having to resort to logarithmic representation.

Abo-Zaid's normalization cancels the effect of changes in contrast, but not the effect of changes in intensity:

$$f'(x, y) = f(x, y) + b$$

In practice, we often experience a combination:

$$f'(x, y) = cf(x, y) + b$$

## 4 Orthogonal moments

We have seen that non-orthogonal moments, e.g. the Cartesian moments using a monomial basis set  $x^p y^q$ , increase rapidly in range as the order increases. Thus, we get highly correlated descriptions, while important differences in objects may be contained within small differences between moments. The net result is that one will need very high numerical precision if moments of high order are used.

Moments produced using orthogonal basis sets have the advantage of needing lower precision to represent differences to the same accuracy as the monomial basis. The orthogonality condition also simplifies the reconstruction of the original function from the generated moments.

Orthogonality means mutually perpendicular: two functions  $y_m$  and  $y_n$  are orthogonal over an interval  $a \leq x \leq b$  if and only if:

$$\int_a^b y_m(x)y_n(x)dx=0; \quad m \neq n$$

Here we are primarily interested in discrete images, so the integrals within the moment descriptors are replaced by summations.

Three such (well established) orthogonal moments are Legendre, Chebyshev and Zernike. Others are Laguerre, Gegenbauer, Jacobi, Hermite, etc.

## 4.1 Legendre moments

The discrete Legendre moments of order  $(m+n)$  of an image function  $f(x,y)$  are defined by

$$\lambda_{mn} = \frac{(2m+1)(2n+1)}{4} \sum_x \sum_y L_m(x) L_n(y) f(x,y), \quad m,n=0,1,2,\dots,\infty$$

$L_m$  and  $L_n$  are the Legendre polynomials of order  $m$  and  $n$ , respectively, and  $f(x,y)$  is the discrete image function, defined over the interval  $[-1,1]$ .

The Legendre polynomial of order  $n$  is defined as:

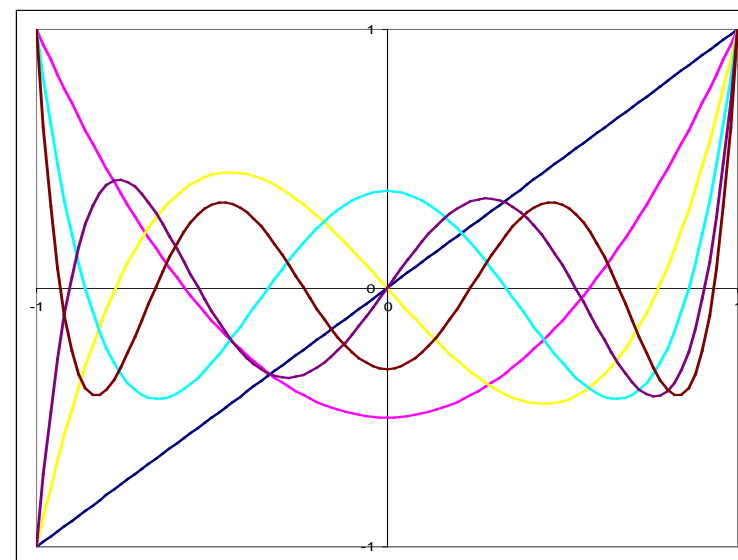
$$L_n(x) = \sum_{j=0}^n a_{nj} x^j, \quad a_{nj} = (-1)^{(n-j)/2} \frac{1}{2^n} \frac{(n-j)!}{\left(\frac{n-j}{2}\right)! \left(\frac{n+j}{2}\right)! j!}, \quad n-j = \text{even}$$

So the first Legendre polynomials and their general recursive relation is given by:

$$\begin{aligned} L_0(x) &= 1 & L_1(x) &= x \\ L_2(x) &= \frac{1}{2}(3x^2 - 1) & L_3(x) &= \frac{1}{2}(5x^3 - 3x) \\ L_4(x) &= \frac{1}{8}(35x^4 - 30x^2 + 3) & L_5(x) &= \frac{1}{8}(63x^5 - 70x^3 + 15x) \\ & \vdots & & \\ L_{n+1}(x) &= \frac{2n+1}{n+1} x L_n(x) - \frac{n}{n+1} L_{n-1}(x) \end{aligned}$$

as illustrated in the figure to the right. It is worth noting that this set of moments is not correlated, as compared to the set of monomials  $x^p$  used for the non-orthogonal Cartesian moments.

The Legendre polynomials are a complete orthogonal basis set defined over the interval  $[-1,1]$ . For orthogonality to exist in the computed moments, the image function has to be defined over the same interval as the basis set. This is achieved by a linear mapping of the shape that is to be analyzed onto this interval.



## 4.2 Chebyshev moments

The discrete Chebyshev moments of order  $(m+n)$  of an image function  $f(x,y)$  are defined by

$$\chi_{mn} = \sum_x \sum_y T_m(x) T_n(y) f(x, y), \quad m, n = 0, 1, 2, \dots, \infty$$

$T_m$  and  $T_n$  are the Chebyshev polynomials of order  $m$  and  $n$ , respectively, and  $f(x,y)$  is the discrete image function, defined over the interval  $[-1,1]$ .

The definition of the Chebyshev polynomials, the first few polynomials, and their recurrence relation are given by

$$T_r(x) = \cos(r \cos^{-1}(x))$$

$$T_0(x) = 1$$

$$T_1(x) = x$$

$$T_2(x) = 2x^2 - 1$$

$$T_3(x) = 4x^3 - 3x$$

$$T_4(x) = 8x^4 - 8x^2 + 1$$

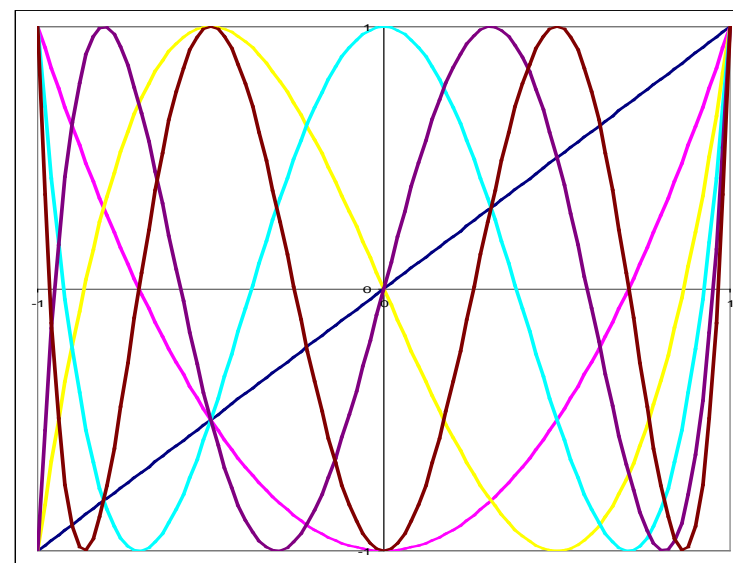
$$T_5(x) = 16x^5 - 20x^3 + 5x$$

$$\vdots$$

$$T_k(x) = 2xT_{k-1}(x) - T_{k-2}(x)$$

The first polynomials are illustrated in the figure to the right.

We notice that the shape of the Chebyshev polynomials is similar to the Legendre polynomials in the central part of the range, while their central and peripheral weights are different.



### 4.3 Zernike moments

The complex Zernike moments are projections of the input image onto the space spanned by the orthogonal V-functions

$$V_{mn}(x, y) = R_{mn}(r) e^{jn\theta}, \quad j = \sqrt{-1}, m \geq 0, |n| \leq m, m - |n| = \text{even}$$

where the orthogonal polynomial  $R_{mn}(x, y)$  is given by

$$R_{mn}(x, y) = \sum_{s=0}^{\frac{m-|n|}{2}} (-1)^s \frac{(m-s)! r^{(m-2s)}}{s! \left(\frac{m+|s|}{2} - s\right)! \left(\frac{m-|s|}{2} - s\right)!}$$

Substituting  $k=(m-2s)$ :

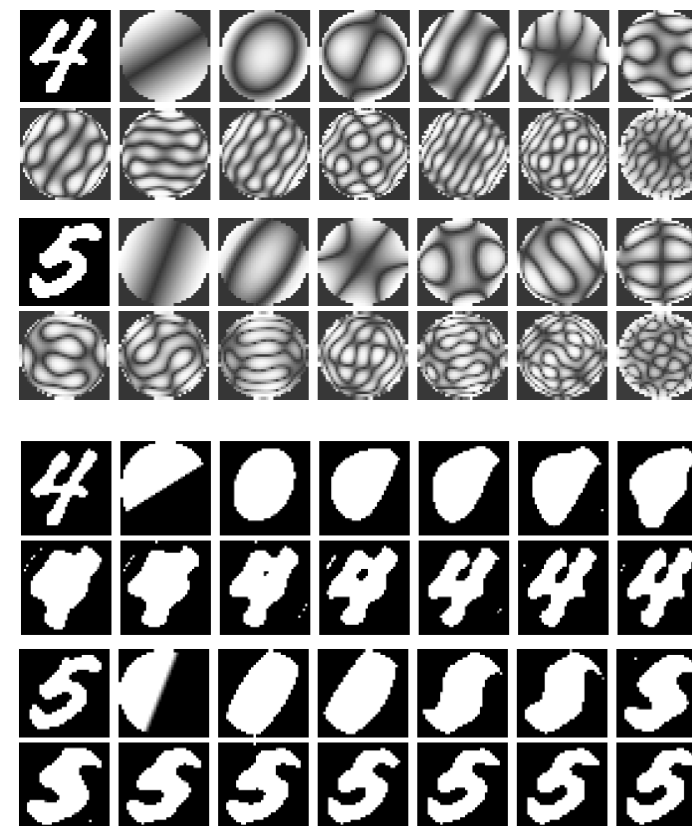
$$R_{mn}(x, y) = \sum_{k=n}^m B_{mnk} r^k, \quad B_{mnk} = (-1)^{\frac{m-k}{2}} \frac{\left(\frac{m+k}{2}\right)!}{\left(\frac{m-k}{2}\right)! \left(\frac{k+n}{2}\right)! \left(\frac{k-n}{2}\right)!}$$

The Zernike moments can be calculated from central Cartesian moments, removing the need for polar mapping, and also removing the dependence on trigonometric functions:

$$Z_{pq} = \frac{p+1}{\pi} \sum_{k=q}^p \sum_{l=0}^t \sum_{m=0}^q (-j)^m \binom{t}{l} \binom{q}{m} B_{pqk} \mu_{(k-2l-q+m)(q+2l-m)}, \quad t = (k-q)/2$$

The object has to be mapped onto the unit disc, either so that the unit circle is within the square area of interest (losing corner information), or such that the square area of interest is within the unit circle (ensuring that all object pixels are included).

The illustrations to the right (from Trier et al., 1996) displays the contributions to Zernike moments of orders up to 13 (top), and the images reconstructed from Zernike moments up to order 13 (bottom), showing that only a few moments are needed in order to distinguish between the two symbols.



## 5 References

- A. Abo-Zaid, O.R. Hinton, and E. Horne, About moment normalization and complex moment descriptors. *Proc. 4<sup>th</sup> Int. Conf. Pattern Recognition*, 399-407, 1988.
- D. Douglas and T. Puecker, Algorithms for the reduction of the number of points required to represent a digitized line or its caricature. *The Canadian Cartographer*, 10, 112-122, 1973.
- H. Freeman, Boundary encoding and processing. In B.S. Lipkin and A. Rosenfeld (eds.), *Picture Processing and Psychopictorics*, 241-266. Academic Press, 1970.
- J. Flusser and T. Suk, Pattern recognition by affine moment invariants. *Pattern Recognition*, 26, 167-174, 1993.
- J. Flusser, On the independence of rotation moment invariants. *Pattern Recognition*, 33, 1405-1410, 2000
- R.M. Haralick and L.G. Shapiro, *Computer and Robot Vision*, Addison-Wesley, 1993.
- Z. Kulpa. Area and perimeter measurement of blobs in discrete binary pictures. *Computer Graphics and Image Processing*, 6, 434-451, 1977.
- B.-C. Li and J. Chen, Fast computation of moment invariants. *Pattern Recognition*, 24, 807-813, 1991.
- O. Trier, A.K. Jain, and T. Taxt, Feature Extraction Methods for Character Recognition-A Survey. *Pattern Recognition*, 29, 641-662, 1996,
- A.M. Vossepoel and A.W.M. Smeulders, Vector code probability and metrication error in the representation of straight lines of finite length. *Comput. Graph. Image Process.*, 20, 347-364, 1982.
- K. Wall and P.E. Danielsson, A fast sequential method for polygonal approximation of digitized curves. *Computer Vision, Graphics, and Image Processing*, 28, 220-227, 1984.

L. Yang, F. Albrechtsen, T. Lønnestad, and P. Grøttum, Methods to estimate areas and perimeters of blob-like objects: A comparison. Proceedings, IAPR Workshop on Machine Vision Applications, pp. 272-276, Kawasaki, Japan, December 13-15, 1994.

L. Yang and F. Albrechtsen, Fast and exact computation of Cartesian geometric moments using discrete Green's theorem. *Pattern Recognition* 29, 1061-1073, 1996.

L. Yang, F. Albrechtsen, and T. Taxt, Fast computation of three-dimensional geometric moments using a discrete divergence theorem and a generalization to higher dimensions. *Graphical Models and Image Processing*, 59, 97-108, 1997.